Proceedings of the 17th World Congress
The International Federation of Automatic Control
Seoul, Korea, July 6-11, 2008

Development of a robust model-based fault diagnosis technique for Reusable Launch Vehicles. A case study

Alexandre Falcoz * **David Henry** * **Ali Zolghadri** *

* *University of Bordeaux I, Automatic control dpt. IMS lab, 351 cours de la libération, 33405 Talence, France (Tel: +33 540003633; e-mail: alexandre.falcoz@laps.ims-bordeaux.fr).*

Abstract: This paper deals with the design of robust Fault Detection and Isolation (FDI) filters for atmospheric re-entry vehicles subjected to actuator faults. The FDI technique is based on carefully chosen linear models of the controlled vehicle about the available on-board reference trajectories. The modelling process allows for both Lateral/directional and longitudinal motions. Design trade-offs are formulated and managed as H_∞/H_- specifications. Nonlinear simulations show the effectiveness of the proposed scheme despite atmospheric disturbances and measurement noises.

1. INTRODUCTION

An integral element of a highly reliable fault-tolerant system for space missions is an efficient Fault Detection and Isolation (FDI) system. In-flight sub-systems employ highly sophisticated fault-tolerant processing mechanisms with redundant capacity to cope with faulty situations. However, some equipment failures which cannot be recovered by the unit itself may take system behavior away from its nominal operation and could lead to flight performances degradation. The fault detection task of in-flight functions is generally based on cross checks, consistency checks and limit-value checking. Monitored variables are checked with regard to certain tolerances of normal values. Alarms are triggered if the thresholds are exceeded. In setting the thresholds, compromises have to be made between the detection size of abnormal deviations and false alarms because of normal fluctuations in the variables. Recent developments in the field of model-based diagnostic offer prospects of an important contribution being made to high level availability with low maintenance cost for future space missions. Good general surveys in the field of model-based FDI can be found in Patton et al. (2000), Isermann (2005), Blanke et al. (2003).

In this paper, an attempt is made to demonstrate the effectiveness of robust model-based FDI techniques for early detection of some out-of-tolerance conditions. The work describes the status of on going research activity undertaken within a collaborative project with ESA (European Space Agency) and EADS Astrium. An attempt is made to show that for robust model-based FDI techniques to be successful, some conditions should be fulfilled about the underlying modeling process. In fact, a well known and classical way to design a model based FDI system is to use a lineralized model of the plant to be supervised. For space or aeronautical applications, decoupled (longitudinal and lateral/directional motions) are very often used see for instance Szaszi et al. (2002). Obviously, this straightforward approach cannot be applied to a re-entry vehicle over its whole flight domain, because of rapidly changing dynamics which depend on reference trajectories to be tracked. Moreover, in a prospect of an onboard implementation, this can lead to a complex global FDI management strategy. Here, we propose to derive reliable linear models which depend on available onboard reference trajectories considering the coupling between the in-plane and out-of plane motions of the vehicle. The solution which will be investigated for the FDI technique and design is based on the work reported in Henry and Zolghadri (2005). It is shown that the robust FDI technique, when associated with an appropriate modeling process could be a powerful and efficient tool for early detection of some out-of-tolerance conditions. This is considered to be the main contribution of this paper.

2. THE CHALLENGE OF FAULT DIAGNOSIS IN ATMOSPHERIC RE-ENTRY

A typical atmospheric reentry for a medium or high L/D vehicle consists in performing three successive flight phases, namely the Hypersonic phase from about 120 km high down to TAEM handover, the TAEM phase from Mach 2 gate down to Mach 0.5 gate and the auto-landing phase from Mach 0.5 gate down to the wheel stop on the runway. After having achieved the hypersonic path, the vehicle initiates the TAEM phase characterized by an entry point called TEP (TAEM entry point), typically defined when crossing Mach 2 gate, and an exit point called NEP (Nominal Exit Point) which is defined in terms of altitude, velocity and distance to the runway. During the reentry scenario, the vehicle is subjected to fast changing and hightly non linear dynamics which are mainly due to the high velocity and the non-linearity of the guidance during the Hypersonic and TAEM paths. This behaviour is partly due to the fast bank reversals which can vary from -180^o to $+180^o$ in short time intervals and the dissipations S-turns performing during the TAEM phase to dissipate the residual kinetic and potential energy of the vehicle.

Because of the restricted flight envelope and low-speed flight regime of the vehicle during the auto-landing phase,

the occurrence of any actuator faults could lead quickly to the vehicle control loss and the time delay to engage recovery actions are therefore very reduced. The design of reliable FDI unit for reentry vehicles appears consequently to be a key feature in the overall system design, as early fault detection of an incipient subsystem abnormality is crucial so as to set up timely safe recovery actions.
In this paper, the goal we purchase is to develop a robust model-based FDI unit being compliant to the stringent operational and flight dynamics constraints, with an acceptable sensitivity level. Two faulty situations occurring during the auto-landing phase are investigated. The first one consists in a movement to the extreme position (runaway) of the right and left wing flap actuators (+30 deg) at a rate of +3.5 deg/s and the second one corresponds to a jamming of the wing flaps at their current values. The faulty scenario corresponding to the runaway occurs at $t = 30$ s and is maintained up to vehicle touchdown on the runway. The scenario relating to the actuator jamming is considered in the time interval of [20s 35s].

3. THE BENCHMARK PLATFORM: HL-20 SIMULATOR

3.1 Description

The vehicle which has been retained in this work is the HL-20 This spacecraft, defined as a component of the proposed Personnel Launch System (PLS) mission , has initially been designed to ensure several manned-space missions including the orbital rescue of astronauts, the International Space Station (ISS) crew exchange or some observations missions. The nonlinear dynamical model of this vehicle is integrated in a simulation tool defined under Matlab/Simulink® environment. It includes atmospheric, wind models and an overall GNC (Guidance, Navigation, Control) architecture dedicated to the auto-landing phase. The HL-20 winged body vehicle consists of an all movable rudder (δ_r), two (right and left) upper and lower body flaps ($\delta_{bful}, \delta_{bfll}, \delta_{bfur}, \delta_{bflr}$) and two trailing edge wing flaps ($\delta_{wfl}, \delta_{wfr}$) which are independently driven by 7 electro mechanical actuators. Deflections relative to these surfaces are collected in the actuator control input vector $u_{act} \in \Re^{7\times 1}$ defined by $u_{act} = [\delta_{wfl}, \delta_{wfr}, \delta_{bful}, \delta_{bfll}, \delta_{bfur}, \delta_{bflr}, \delta_r]^T$. The navigation module consists of an Inertial Measurement Unit (IMU) which is in charge to provide the body angular rates (p, q, r) and lateral accelerations (a_x, a_y, a_z) of the vehicle. Angle-of-attack (α), sideslip (β), True Air Speed velocity (V_{TAS}) and dynamic pressure ($\overline{q}$) are supplied by a flush air data system and information of roll (ϕ) and pitch (θ) angles are obtained via another navigation package.

3.2 HL-20 nonlinear representation

- *Modelling the HL-20 dynamical behavior*

The dynamical behavior of the HL-20 winged body vehicle can be described by a nonlinear state representation:

$$\begin{cases} \dot{x_b} = f(x_b, u) + Ew \\ y = g(x_b) \end{cases} \quad (1)$$

where $x_b = [u_b, v_b, w_b, \phi, \theta, p, q, r]^T$ denotes the state vector of the full aircraft nonlinear model. The state vector is respectively composed of the longitudinal (u_b), lateral (v_b) and vertical (w_b) velocities expressed in the body frame, the roll (ϕ) and pitch (θ) angles and the spacecraft angular rates (p, q, r). y denotes the output vector and consists of the all components of the state vector as well as the angle-of-attack (α) and the sideslip (β). w corresponds to wind and atmospheric turbulences which are modeled using Dryden filters (Johnson (1993)) and acting on the components (u_b, v_b, w_b, p, q, r) of the state vector. u is the control input vector taking into account the actuator dynamics defined by:

$$\begin{cases} \dot{x}_p = A_p x_p + B_p u_{act} \\ u = M_c C_p x_p \end{cases} \quad (2)$$

where (A_p, B_p, C_p) correspond to the state-space matrices of the actuators model and M_c is an allocation matrix in charge to convert the output of the actuators into torques driving the HL-20 dynamics.

For faulty situations, we are interested in the wing-flap actuators jamming and runaway when they are operating. Such faults can be modeled as:

$$\begin{array}{c} u^f_{act}(t) = (I_7 - \chi)u_{act}(t) \\ \chi = diag(\chi_l, \chi_r, 0_5) \end{array} \quad (3)$$

where $\chi_i, i = l, r$ are known. I_7 denotes the identity matrix of dimension 7 and 0_5 is the null matrix of dimension 5. The index f is used to outline the faulty case.

Note that a wing flap actuator jamming corresponds to $\chi_i = 1 - \frac{c}{\delta_{wfi}(t)}$ where c denotes a constant value. The runaway faulty case corresponds to $\chi_i = 1 - \frac{at}{\delta_{wfi}(t)}$ where a is a positive constant corresponding to the wing flaps maximum deflection rate. From (1) and (3), it follows that the HL-20 dynamics can be described by:

$$\dot{x_b} = f(x_b, u) + Ew \quad (4)$$

$$\dot{x}_p = A_p x_p + B_p(I_7 - \chi)u_{act} \quad (5)$$

$$u = M_c C_p x_p \quad (6)$$

$$y = g(x_b) \quad (7)$$

- *Modelling the HL-20 GNC*

The overall GNC architecture implemented in the HL-20 simulator can be described by the block diagram depicted in figure 1 and consists of two coupled loops; the guidance loop and the attitude control loop.

► The guidance loop is in charge of tracking the reference trajectory defined in terms of desired altitude from the runaway treshold by providing roll angle, angle-of-attack and sideslip to the attitude control loop. The guidance algorithm is defined by:

$$\begin{pmatrix} \phi \\ \alpha \\ \beta \end{pmatrix}_{ref} = \int V_{TAS}(t)\varepsilon(t)dt \quad (8)$$

$$\varepsilon = K_G(K_{glide}(x - x_{ref}) - h_m) \quad (9)$$

► The goal of the attitude control loop is to compute the rudder (dr), elevator (de) and aileron (da) authorities

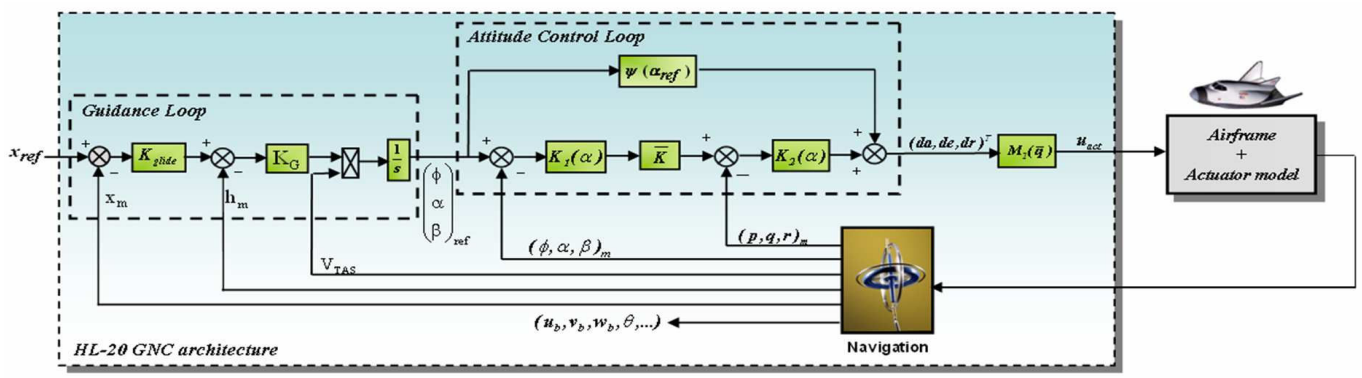

Fig. 1. General setup of the HL-20 simulation tool

corresponding to the guidance input signals. These control signals are given by:

$$\begin{pmatrix} d_a \\ d_e \\ d_r \end{pmatrix} = K_2(\alpha)\overline{K}K_1(\alpha) \begin{pmatrix} \phi_{ref} - \phi_m \\ \alpha_{ref} - \alpha_m \\ \beta_{ref} - \beta_m \end{pmatrix} \quad (10)$$
$$+ \psi(\alpha_{ref}) - K_2(\alpha) \begin{pmatrix} p \\ q \\ r \end{pmatrix}_m$$

where $\psi(\alpha_{ref})$ defines the feed-forward control loop in charge of computing the reference control torques corresponding to the angle-of-attack provided by the guidance loop.

3.3 Augmented LTI model

- *HL-20 modeling*

Coming back to the vehicle dynamics, a linearization around the reference trajectory (Fig. 1) can be performed in order to obtain a LTI (Linear Time Invariant) model. To formulate this problem, first consider the nonlinear equations (4) and (6) and let $\xi x_b = x_b - x_{b_{ref}}$ and $\xi u = u - u_{ref}$ be the tracking errors between the current and reference states and control trajectories. Using a first-order Taylor series expansion, a dynamical error model describing the spacecraft behavior around its reference trajectory can be derived as:

$$\xi\dot{x}_b = A(\theta)\xi x_b + B(\theta)\xi u + Ew \quad (11)$$
$$\xi y = C(\theta)\xi x_b + D(\theta)\xi u \quad (12)$$
$$\dot{x}_p = A_p x_p + B_p(I_7 - \chi)\xi u_{act} \quad (13)$$
$$\xi u = M_c C_p x_p \quad (14)$$

ξu_{act} denotes the tracking error between the current and reference control input trajectories of the 7 control aerosurfaces. A, B, C, D are known state matrices of appropriate dimensions and $\theta = (\theta_1, ..., \theta_n)$ defines a bounded time-varying parameter vector depending on $x_{b_{ref}}$ and u_{ref} such as $\underline{\theta_i} < \theta_i < \overline{\theta_i}$ for $i = 1, ..., n$. Here, considering the slow dynamics of the vehicle during the auto-landing phase (no out-of-plane manoeuvre is to be performed), it is assumed that θ does not really vary so that it can be fixed to its nominal value. Then, it follows from (11) to (14) that the HL-20 vehicle dynamics can be described by the following state space representation during the auto-landing phase:

$$\xi\dot{x}_b = A\xi x_b + B\xi u + Ew \quad (15)$$
$$\xi y = C\xi x_b + D\xi u \quad (16)$$
$$\dot{x}_p = A_p x_p + B_p(I_7 - \chi)\xi u_{act} \quad (17)$$
$$\xi u = M_c C_p x_p \quad (18)$$

Now, using an approximation of the actuator fault model (3) in terms of additive fault type, the equation (17) can be rewritten as:

$$\dot{x}_p = A_p x_p + B_p \xi u_{act} + \sum_{i=1}^{2} F_i f_i \quad (19)$$

where K_i $i = 1, 2$ denotes a distribution matrix associated with the i^{th} fault f_i. Note that this approximation makes sense as long as the HL-20 control law keeps stability in faulty situations. Finally, from (15), (16), (18) and (19) it follows that the HL-20 winged body vehicle can be written by:

$$\xi y = P(s) \begin{pmatrix} w \\ f_i \\ \xi u_{act} \end{pmatrix} + n \quad (20)$$

where n is the measurement noises.
In this formulation, it is assumed that (without loss of generality) K_i, $i = 1, 2$ are monic and the unobservable subspace of (C, A) associated with P does not intersect the image of K_i. The above assumption is necessary to ensure fault detectability (see Massoumia (1986) for more details).

- *Attitude control loop*

As already mentioned, the flight control system consists of two separated gain scheduling-based controllers $K_1(\alpha)$ and $K_2(\alpha)$. These two controllers were provided initially by Look Up Tables depending on the reference angle-of-attack given by the guidance loop. Since it is assumed that α varies slowly and in a small range during the auto-landing phase, the numerical expression of $K_1(\alpha)$, $K_2(\alpha)$ and $\psi(\alpha_{ref})$ can be approximated by fixing α and α_{ref} to there mean value. As depicted in figure 1, a pressure dependent allocation matrix $M_2(\overline{q})$ is in charge to convert the computed control torques into the actuator control input vector. Similarly, due to the fact that $\bar{q}$ does not vary in a large range during the considered reentry phase, $M_2(\overline{q})$ is fixed to a constant matrix. Finally since $\overline{K}$ is a 2^{nd} order linear controller designed to keep stability an performances

(see Fig.1), it follows that the HL-20 attitude control loop can be modeled as a linear multivariable controller $K(s)$ defined by:

$$K(s) = M_1(\overline{q})K_2\bar{K}(s)K_1(\Delta\Phi, \Delta\alpha, \Delta\beta)^T - M_1(\overline{q})K_2(p,q,r)^T \quad (21)$$

Finally, taking into account (20) and (21) it follows that the overall setup described in figure 1 can be modeled as illustrated in figure 2. This model describes the dynamic of the HL-20 around the auto-landing trajectory defined by $(\phi_{ref}, \alpha_{ref}, \beta_{ref})$. Using some linear algebra manipulations, it can be shown that the model depicted in figure 4 can be re-casted as follows:

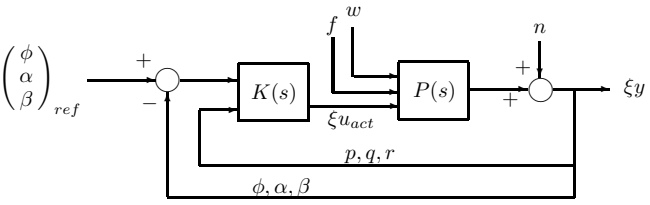

Fig. 2. Block diagram of the overall HL-20 simulation tool

$$\xi y = \overline{P}(s)(w, n, f, \phi_{ref}, \alpha_{ref}, \beta_{ref}, \xi u_{act}) \quad (22)$$

where $\overline{P}$ is deduced from (20) and (21). This form will be suitable for the FDI design procedure presented in Henry and Zolghadri (2005). Linear simulations versus nonlinear one have finally been performed to validate the transient and steady behavior of the linearized model. For the sake of place, the temporal simulations are not presented here.

4. FDI TECHNIQUE AND DESIGN

In this section, the problem of designing a Fault Detection unit scheme able to detect the underlying fault f (see equation (3)) is addressed. The design method is based on the methodology proposed in Henry and Zolghadri (2005). The strategy consists of a bank of two fault detection filters that are designed so that a given filter is made robust against measurement noises n, winds and atmospheric turbulences w, the guidance reference signals $(\phi_{ref}, \alpha_{ref}, \beta_{ref})$ and simultaneously sensitive to a given fault f_i. Design objectives are formulated by means of H_∞/H_- specifications. In the following, an earnest attempt is made to avoid duplicating materials presented in Henry and Zolghadri (2005). Consequently, the main purpose of this section is to clearly show how the results presented in the previous section can be used within the proposed FDI technique. The interested reader can refer to Henry and Zolghadri (2005) for further details and proofs about the FDI method.

4.1 Problem formulation

Let us consider the fault detection design problem depicted in figure 3 where P_1 is derived from figure 2 using linear algebra. K denotes the attitude control law defined by (21). The notation $i = 1, 2$ is used to outline the fact that we need to design two fault detection filters. Some manipulations on P_1, K, M_y and M_u allow us to recast the setup depicted in Fig.3.a into the diagram shown on Fig.3.b, where the augmented disturbances vector d is

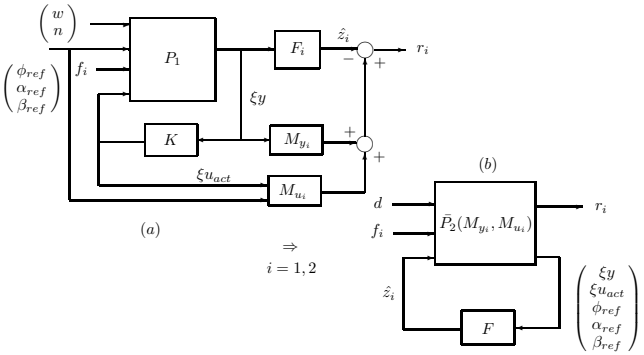

Fig. 3. General setup of the FDI/LTI filter design problem

defined according to $d = (\phi_{ref}, \alpha_{ref}, \beta_{ref}, w, n)^T$. $\hat{z}$ is an estimation of $z_i = M_{y_i}\xi y + M_{u_i}(\xi u_{act}^T, \phi_{ref}, \alpha_{ref}, \beta_{ref})^T$ a subset of available input/output signals. M_{y_i} and M_{u_i} are two (static) structuration matrices of appropriate dimension. The role of M_{y_i} and M_{u_i} is to merge optimally the available measurement and control signals to build the residual r defined by:

$$r_i = z_i - \hat{z}_i = M_{y_i}\xi y + M_{u_i}\xi u_{act} - F_i(s)\begin{pmatrix} \xi y \\ (\xi u_{act}^T, \phi_{ref}, \alpha_{ref}, \beta_{ref})^T \end{pmatrix} i = 1, 2 \quad (23)$$

For clarity, the index "i" is omitted in the following.
The robustness requirement against d can be formulated in the H_∞ framework as the problem of finding F that minimizes the worst case residual r to disturbances d, that is:

$$\min_{(M_y, M_u, F)} ||T_{d\to r}||_\infty \quad (24)$$

or equivalently

$$\begin{array}{ll} \min\limits_{(M_y, M_u, F)} & \gamma_1 \\ \text{s.t.} & ||T_{d\to r}||_\infty < \gamma_1 \end{array} \quad (25)$$

where $T_{d\to r}$ is the transfer function from d to r. Here $||\mathbf{P}||_\infty = \sup_\omega \overline{\sigma}(\mathbf{P}(j\omega))$ is the H_∞-norm of $\mathbf{P}$ and $\overline{\sigma}(\bullet)$ denotes the maximum singular value. In other words, (24) is the robustness specification of the residual r against the measurement noises, the winds and atmospheric turbulences and the guidance references.

The fault sensitivity requirement can be expressed as a worst-case criterion for the sensitivity of the residual signal to faults that can be formulated in the H_- setting:

$$\max_{(M_y, M_u, F)} ||T_{f\to r}||_- \quad (26)$$

or equivalently

$$\begin{array}{ll} \max\limits_{(M_y, M_u, F)} & \gamma_2 \\ \text{s.t.} & ||T_{f\to r}||_- > \gamma_2 \end{array} \quad (27)$$

In this formulation, $||\mathbf{M}||_- = \inf\limits_{\omega\in\Omega} \underline{\sigma}(\mathbf{M}(j\omega))$, $\Omega = [\omega_1\,;\,\omega_2]$ denotes the H_- norm of $\mathbf{M}$ introduced in Chen and Patton (1999). $\underline{\sigma}(\mathbf{M}(j\omega))$ denotes the minimum non-zero singular value of matrix $\mathbf{M}(j\omega)$ and $\Omega = [\omega_1\,;\,\omega_2]$ the evaluated frequency range in which $\underline{\sigma}(\mathbf{M}(j\omega)) \neq 0$.

To solve (24) and (26), the proposed in Henry and Zolghadri (2005) consists in introducing two shaping filters W_d and W_f to express respectively the robustness objectives and the fault sensitivity requirements in terms of loop shapes, i.e., of desired gain responses for the appropriate

closed-loop transfers. To proceed, define two shaping filters W_d and W_f such that

$$||W_d||_\infty \leq \gamma_1 \ ||W_f||_- \geq \gamma_2. \tag{28}$$

Assume that W_d and W_f are invertible (this can be done without loss of of generality because it is always possible to add zeros in W_d and W_f to make them invertible), W_d and W_f are also defined in order to tune the gain responses for, respectively, $T_{d\to r}$ and $T_{f\to r}$. Then, if the condition

$$||T_{d\to r}W_d^{-1}||_\infty < 1 \tag{29}$$

is satisfied, the robustness specification against d yields.

To transform the fault sensitivity objective into a H_∞ constraint, the following lemma (Henry and Zolghadri (2005)) can be used. The proof of this lemma is omitted here and the interested reader can refer to Henry and Zolghadri (2005) for further details.

Lemma 1:

Let W_F be a right invertible transfer matrix so that $||W_f||_- = \frac{\gamma_2}{\lambda}||W_F||_-$ and $||W_F||_- > \lambda$, where $\lambda = 1+\gamma_2$. Define the signal $\tilde{r}$ such that $\tilde{r} = r - W_F(s)f$ (see Fig.6). Then a sufficient condition for $||T_{f\to r}||_- \geq \gamma_2$ to hold, is:

$$||T_{f\to r} - W_F||_\infty < 1 \Leftrightarrow ||T_{f\to\tilde{r}}||_\infty < 1 \tag{30}$$

where $T_{f\to\tilde{r}}$ denotes the closed-loop transfer between $\tilde{r}$ and f.

This lemma allows the formulation of the min-max optimisation problem as a maximum gain optimisation problem. Following equations (29) and (30), the design problem can be formulated within the H_∞ setting by combining (29) and (30) into a unique H_∞ requirement. Also, including γ_2, λ, and the weighting functions W_d^{-1} and W_F into the model $\bar{P}_2$ (see Fig.3.b), a new model $\tilde{P}(M_y, M_u)$, as depicted in figure 4, depending on the residual structuration matrices M_y and M_u can be derived so that:

$$\begin{pmatrix} r \\ \tilde{r} \end{pmatrix} = \left(\tilde{P}(M_y, M_u, s) \star F(s)\right)\tilde{d} \tag{31}$$

where $\star$ denotes the redheffer product. $\tilde{d}$ is a fictitious signals generating d through W_d. Then, a sufficient condition for specifications (24) and (26) to hold is:

$$\left\| \left(\tilde{P}(M_y, M_u) \star F\right) \right\|_\infty \leq 1 \tag{32}$$

This specification seems to be a standard H_∞ equation.

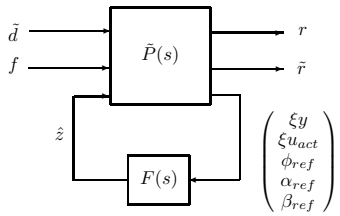

Fig. 4. General FDI synthesis scheme

In fact, this is not the case since the transfer $\tilde{P}(M_y, M_u)$ depends on M_y and M_u that are unknown. A solution may be to choose heuristically M_y and M_u. However, as it has been outlined by several authors (see Chen and Patton (1999); Henry and Zolghadri (2005) for instance), there is no guarantee for the solution to be optimal. The following proposition allows us to solve this problem. A complete proof of this proposition can be found in Henry and Zolghadri (2005):

Proposition 1:

Assume that $\tilde{P}(M_y, M_u)$ admits the following state space representation:

$$\tilde{P}: \begin{cases} \dot{x} = Ax + B_1 d + B_2\hat{z} \\ \begin{pmatrix} r^T & \tilde{r}^T \end{pmatrix}^T = C_1(M_y, M_u)x + D_{11}(M_y, M_u)... \\ \qquad\qquad ...(\tilde{d}^T f^T)^T + D_{12}\hat{z} \\ \begin{pmatrix} \xi y^T & \xi u_{act}^T \end{pmatrix}^T = C_2 x + D_{21}(\tilde{d}^T f^T)^T + D_{22}\hat{z} \end{cases} \tag{33}$$

where $A, B_1, B_2, C_1(M_y, M_u), C_2, D_{11}(M_y, M_u), D_{12}, D_{21}$ and D_{22} are matrices of adequate dimensions. Let W denotes an orthonormal basis of the null space of $(\tilde{C}_2^T \tilde{D}_{21}^T)$. Then F, M_y and M_u satisfy (32) if and only if there exist $\gamma < 1$ and two symmetric matrices $R > 0$ and $S > 0$ solving the SDP (Semi Definite Programming) problem:

$$\begin{pmatrix} AR + RA^T & B_1 \\ B_1^T & -\gamma I \end{pmatrix} < 0 \tag{34}$$

$$\left(\begin{array}{c|c} \mathcal{W} & 0 \\ \hline 0 & I \end{array}\right)^T ... \\ ... \left(\begin{array}{cc|c} A^T S + SA & SB_1 & C_1^T(M_y, M_u) \\ B_1^T S & -\gamma I & D_{11}^T(M_y, M_u) \\ \hline C_1(M_y, M_u) & D_{11}(M_y, M_u) & -\gamma I \end{array}\right) ... \\ ... \left(\begin{array}{c|c} \mathcal{W} & 0 \\ \hline 0 & I \end{array}\right) < 0 \tag{35}$$

$$\begin{pmatrix} R & I \\ I & S \end{pmatrix} \geq 0 \tag{36}$$

The filter F is then computed from the unique solution (R, S, M_y, M_u, γ).

5. EXPERIMENTAL RESULTS

The two diagnosis filters F_1 and F_2 have been designed so that the two residual r_1 and r_2 are respectively sensitive to the right and left wing flap actuator faults and simultaneously robust with respect to the guidance signals, measurement noises and atmospheric disturbances (wind gust, turbulence, wind shear).

Following the method described in section 4, the robustness objectives are expressed in terms of shaping filters. Here, four shaping filters are required, i.e. W_n to deal with the robustness constraint against n, $W_g = diag(W_{\phi_{ref}}, W_{\alpha_{ref}}, W_{\beta_{ref}})$ to deal with robustness against the guidance signals and $W_w = diag(W_{uw}, W_{vw}, W_{ww}, W_{pw}, W_{qw}, W_{rw})$ to deal with robustness against the atmospheric disturbances. Finally, W_F is defined to model the fault sensitivity specifications.

Since it is assumed that the energy content of $n(t)$ is located in the high frequencies, W_n is chosen as a low pass filter such as:

$$W_n(s) = \gamma_n \frac{1 + 0.005s}{1 + 0.0125s} I_{10} \tag{37}$$

where γ_n is a positive constant introduced to manage the gain of W_n. Without any frequency information about the robustness requirement against the guidance signals, W_g is chosen to be a constant matrix i.e.

$$W_g = \gamma_g I_3 \tag{38}$$

For the atmospheric disturbances, three wind models for the wind shear, turbulence and wind gust are implemented in the simulator. These models depend on the current vehicle altitude and true air speed velocity. To deal with the robustness objectives against these disturbances, W_w has been chosen as a constant matrix. It is obvious that this choice brings a certain degree of pessimism into the design but it allows us to ensure the residual robustness against atmospheric disturbances with respect to a wide range of unknown inputs (i.e. large frequency range):

$$W_w = \gamma_w I_6 \tag{39}$$

For fault sensitivity, we consider that the actuator faults manifest themselves in the low frequencies. This boils down to fixing W_{F_i} as a first-order low-pass filter at cutting frequency ω_{f_i} such as.

$$W_{F_i}(s) = \lambda_{f_i} \frac{1}{1 + \frac{s}{\omega_{f_i}}} \tag{40}$$

$\lambda_{f_i} = 1 + \gamma_{2i}$, $i = 1, 2$
The 2 fault detection filters and the residual structuration matrices M_{yi}, M_{ui}, for $i = 1, 2$ are then computed following ***lemma 1*** and ***proposition 1***. All LMI-related computation have been performed using the Matlab's free package SDPT3. The parameters γ_n, γ_g, γ_w, γ_{2i} and w_{fi} $i = 1, 2$ are optimized by performing an iterative refinement. Recall that the goal is to minimize the effects of disturbances on the residuals and maximizing the effects of faults on r (see (24) and (26)). This implies of course a trade-off between γ_n, γ_g, γ_w, γ_{2i} and w_{fi} $i = 1, 2$. The numerical values of the computed parameters are listed in Table 1.

Filter	γ_n	γ_g	γ_w	γ_2
$F_1(s)$	0.05	$2.2e^{-3}$	0.005	0.5
$F_1(s)$	0.01	$4e^{-3}$	0.005	0.45

Table 1. FDI unit computed parameters

5.1 Nonlinear simulations

The 2 diagnosis filters are converted to discrete-time using a Tustin approximation (sampling period of 10 ms) and implemented within the HL-20 nonlinear simulator. The simulation has been carried out all during the auto-landing phase scenario. Figure 5 illustrates the residuals behavior $r_i(t), i = 1, 2$ in fault free and faulty situations for the two considered faulty scenarios (i.e. wing flap actuator jamming and runaway). To make a final decision about the fault, a sequential Wald test is also implemented within the simulation environment. The probability of non-detection (P_{ND}) and false alarm (P_F) have together been fixed to 10^{-6}. As expected, it can be seen that the actuator faulty scenarios are successfully detected after a very short delay (30 ms) in spite of measurement noises, atmospheric disturbances and whatever the signals provided by the guidance loop.

6. CONCLUDING REMARKS

This paper addressed the fault diagnosis task for a re-entry vehicle during the auto-landing phase. A Fault Detection (FD) scheme is proposed to generate residuals robust against disturbances coming from guidance control loop, measurement noises and wind while guaranteeing high fault sensitivity level. The FD strategy consists in two dedicated H_∞/H_- fault detection filters dedicated to the right and left wing flap actuators. Nonlinear simulations have shown that all the considered faulty scenarios can successfully be detected.

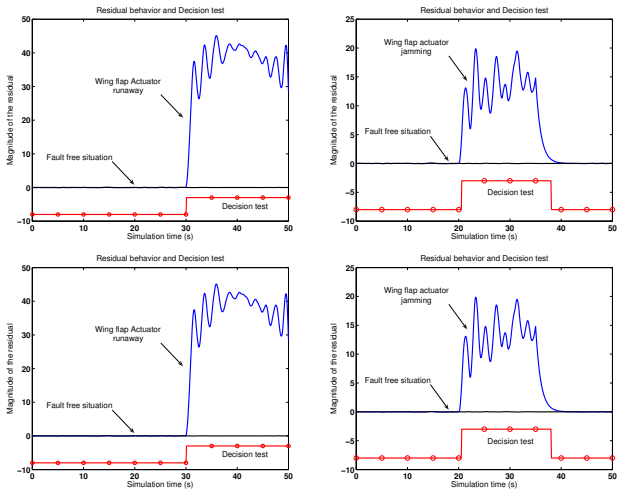

Fig. 5. Behavior of the left (top) and right (bottom) wing flap residuals and the decision test

7. ACKNOWLEDGEMENTS

The authors would like to thank Eric Bornschlegl from European Space Agency and et Martine Ganet-Schoeller from EADS Astrium for their helpful and valuable comments. The financial support by European Space Agency and EADS Astrium is gratefully acknowledged.

REFERENCES

M. Blanke, M. Kinnaert, M. Lunze, and M. Stareoswiecki. *Diagnosis and fault tolerant control*. Springer, New York, 2003.

J. Chen and R.J. Patton. *Robust model-based fault diagnosis for dynamic systems*. Kluwer Academic Publishers, 1999.

D. Henry and A. Zolghadri. Design and analysis of robust residual generators for systems under feedback control. *Automatica*, 41:251–264, 2005.

R. Isermann. Model-based fault detection and diagnosis-status and applications. *Annual review in Control*, 29: 71–85, 2005.

D.L Johnson. Terrestrial environment (climatic) criteria guidelines for use in aerospace vehicle development. *NASA Technical Memorandum 4511,1993*, 1993.

M.A. Massoumia. A geometric approach to the synthesis of failure detection filters. *IEEE Transactions of Automatic Control*, 31(9):839–846, 1986.

R. Patton, P. Frank, and R. Clark. Issues of fault diagnosis for dynamic systems. *International Journal of Robust and Nonlinear Control*, 10(14):1209–1236, 2000.

Istvan Szaszi, Subhabrata Ganguli, Andres Marcos, Gary J. Balas, and Jozsef Bokor. Application of fdi to a nonlinear boeing-747 aircraft. In *Proceedings of the 10th Mediterranean Conference on Control and Automation*, Lisbon, Portugal, 2002. MED2002.